J. Fluid Mech. (1987), *vol.* 184, *pp.* 157–181
Printed in Great Britain

Natural convection about a heated horizontal cylinder in a porous medium

By D. B. INGHAM
Department of Applied Mathematical Studies, The University of Leeds, Leeds LS2 9JT, West Yorkshire, UK

AND I. POP
Faculty of Mathematics, University of Cluj, Cluj, Romania

(Received 4 November 1986)

The natural convection from a heated circular cylinder in an unbounded region of porous medium is investigated for the full range of Rayleigh numbers. At small Rayleigh numbers a qualitative solution is obtained and at large Rayleigh numbers the second-order boundary-layer solution is found that takes into account the first-order plume solution. In order to find the solution at finite Rayleigh numbers the two governing coupled, nonlinear, elliptic partial differential equations are expressed in finite-difference form using a specialized technique which is second-order accurate everywhere. Further, methods are devised which deal with the plume and infinity boundary conditions. Although numerical results are presented for Rayleigh numbers up to 400 solutions of the finite-difference equations can be obtained for higher values of the Rayleigh numbers but in these cases the mesh size used is too large to adequately deal with the developing boundary-layer on the cylinder and the plume.

The numerical results show how the theories at both low and high Rayleigh numbers are approached. The plume solution which develops with increasing Rayleigh number agrees with that predicted by the theory presented using the boundary-layer approximation. No separation of the flow at the top of the cylinder is found and there are no indications that it will appear at higher values of the Rayleigh number. The results presented here give reasonable agreement with the existing experimental results for Rayleigh numbers of order unity. However as the Rayleigh number increases to order 10^2 there is a large discrepancy between the theoretical and experimental results and this is because at these higher values of the Rayleigh number the Darcy approximation has been violated in the experimental results. This indicates the severe limitations of some of the existing theories which use boundary-layer analyses and the Darcy approximation for flows in a porous medium. The application of Darcy's law requires that the size of the pores be much smaller than the scale of the bulk flow and inertial and thermal lengthscales.

1. Introduction

The study of isothermal flow through a porous medium dates back to the work of Darcy (1856) who performed his well-known experiments on flow through a sand column and he postulated what has now become known as Darcy's law. Since this pioneering work the theory has been applied to a number of disciplines including

groundwater hydrology, soil mechanics, petroleum reservoir engineering, chemical process engineering.

The early theoretical work on heat transfer in a porous medium was focused on the onset of natural convection and cellular convection in rectangular enclosures with heating from below. However, recently there has been an increasing interest in the natural convection in a porous medium external to heated surfaces and bodies. In many papers it has been assumed that the Rayleigh number is large and therefore the boundary-layer approximations have been employed. Usually similarity solutions have been obtained in these situations for two-dimensional and axisymmetric bodies, see Merkin (1979). Further higher-order boundary-layer theories have been developed in order to assess the accuracy of the boundary-layer approximation but these analyses have been restricted to only very simple planar geometries, see for example Cheng & Hsu (1984). Very few papers have investigated the situation when the Rayleigh number is small but Yamamoto (1974) did obtain an asymptotic solution for small values of the Grashof number for the natural convection about a heated sphere in a porous medium. However, his solution has the defect that the pressure does not remain bounded at large distances from the sphere. Caltagirone (1976) investigated the natural convection in a porous medium which is bounded by two concentric horizontal cylinders, whilst Burns & Tien (1979) also considered flow between concentric spheres. The governing equations were solved at finite Rayleigh numbers by the use of a finite-difference scheme, whilst for small Rayleigh numbers a regular perturbation analysis was presented in which the stream function and temperature are expanded in a power series of the Rayleigh number. An increasing number of experimental investigations are now being performed in different geometries and for a wide range of Rayleigh numbers and some of these have been reviewed by Cheng (1985) and Nield (1985).

In recent years several analytical studies have been performed for the steady two-dimensional natural convection about an infinitely long horizontal isothermal cylinder embedded in a porous medium of infinite extent, the cylinder being maintained at a temperature T_w and the surroundings at T_∞. In most of these studies it has been assumed that Darcy's law holds and the boundary-layer equations are appropriate. A curvilinear orthogonal coordinate system has been employed and the gravitational force normal to the heated surface assumed negligible. Under these assumptions Hardee (1976) used an integral method and predicted that the Nusselt number Nu varied with the Darcy-modified Rayleigh number Ra as

$$Nu = 0.465 Ra^{\frac{1}{2}},$$

where $Ra = \kappa g \beta \rho_\infty D(T_w - T_\infty)/(\mu\alpha)$. Here κ is the permeability, g the gravitational constant, β the coefficient of volumetric expansion of the fluid, D the diameter of the cylinder, α the effective diffusivity and μ the dynamic viscosity of the fluid.

Using a similarity method, Merkin (1979) obtained solutions for the natural convection porous boundary layers adjacent to axisymmetric and two-dimensional bodies of arbitrary shape. For the particular case of a horizontal isothermal circular cylinder one obtains

$$Nu = 0.565 Ra^{\frac{1}{2}}.$$

In order to test these theories, Fand, Steinberger & Cheng (1986) performed an experimental investigation of heat transfer by natural convection from a horizontal circular cylinder embedded in a porous medium which consists of randomly packed glass spheres saturated by either water or silicone oil. They showed that the overall

range of the Rayleigh number can be divided into two subregions, called 'low' and 'high', in each of which the Nusselt number behaves differently. It was demonstrated that the low-Ra region corresponds to Darcy flow. However in the high-Ra region the flow is non-Darcian and the flow model of Forchheimer (1901) is appropriate. In the limiting case of very high Rayleigh number in which the boundary-layer equations may be assumed to hold Ingham (1987) modified the theory of Merkin (1979) in order to deal with the non-Darcian effects. He found that

$$Nu \propto Ra^{\frac{1}{4}}\left(\frac{\nu D}{\chi\alpha}\right)^{\frac{1}{2}}$$

where χ is the Forchheimer coefficient. This shows that the Nusselt number is proportional to the Rayleigh number raised to the power $\frac{1}{4}$ for non-Darcy flow whereas it is to the $\frac{1}{2}$ power for Darcy flow.

In this paper the natural convection about a heated horizontal cylinder in a porous medium is investigated under the assumption of the flow being governed by Darcy's law. Theoretical results are obtained for small and large values of the Rayleigh number and the limiting solutions matched by employing a numerical technique for moderate values of the Rayleigh number. When employing the numerical technique there is no difficulty in extending the work to include for example non-Darcy flow, boundary effects, thermal dispersion, etc. However, the main aim of the present paper is to produce a complete picture for Darcian flow only.

When the Rayleigh number is very small there does not exist a simple analytical solution corresponding to $Ra \equiv 0$. This contrasts with the problem of a sphere, rather than a cylinder, where Yamamoto (1974) was able to obtain an asymptotic solution for small values of Rayleigh number. The problem encountered in this paper is analogous to that experienced by Mahony (1957) when considering the heat transfer from an isothermal horizontal cylinder at small values of the Grashof number.

At large values of the Rayleigh number the boundary-layer approximation can be made and the flow in the vicinity of the cylinder is that predicted by Merkin (1979). However a wake develops above the cylinder and this can be modelled at large distances as a plume above a horizontal line source of heat. When dealing with the second-order boundary layer on the cylinder, the outer flow solution must first be determined. In order to perform this calculation the first-order flow in both the boundary layer and the plume has to be determined. This has been performed and the second-order boundary-layer solution on the cylinder determined.

The numerical method presented here is based on the use of specialized techniques to obtain an approximating set of finite-difference equations to the full partial differential equations which govern the flow. The origins of the method date back to Allen & Southwell (1955), Dennis (1960, 1973), Roscoe (1975, 1976) and Spalding (1972). Unfortunately, these methods involve exponential coefficients and the associated matrices are not always diagonally dominant. However it is possible to expand these exponential functions in a series and hence both of these difficulties can be removed while still maintaining second-order accuracy following the method of Dennis & Hudson (1978) and Dennis, Ingham & Cook (1979). The resulting finite-difference equations may then be solved using standard iterative techniques. Results have been obtained for several mesh sizes and h^2 extrapolation employed.

Solving unbounded problems using finite-difference and finite-element techniques has always been difficult because of the implementation of the appropriate boundary conditions at infinity. For steady flow past a circular cylinder, Fornberg (1980) has performed a thorough investigation of the possible boundary conditions at infinity

and postulated conditions that he believes lead to the most accurate solutions. However for this problem the vorticity tends to zero and the stream function to a bounded value. Kuehn & Goldstein (1980) when solving the full Navier–Stokes equations for laminar convection about a horizontal isothermal circular cylinder treats the infinity boundary condition in two parts – one with the fluid coming into the solution domain, the other with the fluid leaving. The fluid is assumed to approach the cylinder radially at ambient fluid temperature whilst it is assumed that it leaves radially in the plume with negligible radial temperature gradient. They state that the position at which the outer boundary condition has been applied has an effect on the results if it is not set far enough from the surface of the cylinder and this distance was varied from one to twenty diameters. Apart from that in applying the outer boundary condition at a finite distance from the cylinder one of the major difficulties in obtaining an accurate solution is the existence of the plume. Although within the plume the temperature decays inversely with distance from the centre of the cylinder to the power $\frac{3}{5}$, the stream function increases with this distance to the power $\frac{3}{5}$. It is this unboundedness in the stream function at large distances that makes it so difficult in this problem to obtain accurate results at large values of the Grashof number. A similar phenomenon exists in the problem under consideration here and a method is developed in order to eliminate this difficulty.

Numerical results are presented in this paper for values of the Rayleigh number in the range 10^{-2} to 400 and in all cases h^2 extrapolation is used. For Ra of order unity the numerical results are in reasonable agreement with the experimental results of Fand *et al.* (1986). At very small values of the Rayleigh number it is very difficult to obtain accurate solutions, whereas the asymptotic solution for small values of the Rayleigh number is only valid for $-\log Ra \gg 1$. At large values of the Rayleigh number the numerical results tend to the boundary-layer solution but disagree with the experimental results of Fand *et al.* (1986). However at large values of the Rayleigh number the experimental results correspond to large values of the local Reynolds number and hence the Darcy approximation will no longer be valid.

The numerical results show evidence of the development of the plume in which the fluid near the cylinder moves towards the top of the cylinder and is expelled in a radial jet. This phenomenon has been observed experimentally by Cheng (1985). In the present calculations the plume region is found to narrow with increasing Rayleigh number with a corresponding increase of the radial component of velocity. As the Rayleigh number increases it is shown that the plume solution is approached.

Recently there has been a great deal of interest shown in situations where two streams of fluid, emanating from two distinct regions, meet and then proceed in a single flow. In the case of a heated horizontal circular cylinder in a porous medium the two boundary layers grow from the lowest generator and collide at the uppermost generator. For the problem of a sphere rotating with constant angular velocity in a fluid otherwise at rest, the boundary layers grow from the poles and collide at the equator. Nigam (1954) proposed a solution in which the boundary layers were empty of fluid at the equator, but Banks (1965) and Stewartson (1958) showed that this situation was not possible. Banks (1976) also attempted an inviscid theory as proposed by Stewartson (1958) but concluded that the interaction at the equator was a viscous problem. Smith & Duck (1977) postulated that there is a large (compared with the boundary-layer thickness) recirculating region near the equator. In the range of Rayleigh numbers considered here, there is no evidence that the collision of the boundary layers at the top of the cylinder gives rise to a recirculating region.

2. Equations

We investigate the steady-state natural convection about a heated horizontal circular cylinder of radius a embedded in an unlimited mass of uniform porous medium with constant permeability κ. The temperature of the cylinder is T_w and that of the ambient medium is T_∞. The porous medium is assumed to be an effective continuum and this is generally valid for systems where the non-dimensional pore space, the square of which is qualitatively represented by the Darcy number, $\kappa/(\text{radial distance between inner and outer boundaries})^2$, is much less than unity. Darcy's law then adequately describes the transfer of momentum provided that the Reynolds number based on the pore diameter is less than about unity, see Muskat (1946), Scheidegger (1974), Beavers & Sparrow (1969) and Fand *et al.* (1986), so that inertial effects are negligible. It is further assumed that the convective fluid and porous medium are in local thermal equilibrium, the properties of the fluid and porous medium are constant and isotropic, the Boussinesq approximation is applicable and the thermal dispersion is negligible. The convective flow is assumed to be moving upwards while gravity acts vertically downwards. We take cylindrical polar coordinates with the axis of the cylinder at $r' = 0$ and $\theta = 0$ as the downward vertical and assume all quantities are independent of z'.

The governing equations can be written in dimensionless form, see Yih (1965),

$$\nabla \cdot \boldsymbol{v} = 0, \tag{1}$$

$$\boldsymbol{v} = -\nabla p - T\boldsymbol{k}, \tag{2}$$

$$\boldsymbol{v} \cdot \nabla T = \frac{1}{Ra} \nabla^2 T, \tag{3}$$

where $(g\beta(T_w - T_\infty)\rho_0 \kappa/\mu)\boldsymbol{v}$ is the velocity vector, $(ag\beta(T_w - T_\infty)\rho_0 \kappa/\mu)p$ is the pressure, $T_0 + (T_w - T_\infty)T$ is the temperature. Coordinates are non-dimensionalized by using a as the lengthscale, $\boldsymbol{k} = (\cos\theta, -\sin\theta, 0)$ is a unit vector in the direction of gravity and $Ra = g\beta(T_w - T_\infty)\rho_0 \kappa a/(\mu\alpha)$ is the Rayleigh number. Here μ is the dynamic viscosity of the fluid, ρ_0 the density of the convective fluid, α the effective thermal diffusivity, β the coefficient of volumetric expansion of the fluid and g the acceleration due to gravity.

Introducing the stream function in order to satisfy (1), eliminating the pressure from (2) and writing the resulting equation in cylindrical polar coordinates leads to the equations

$$\frac{\partial^2 \psi}{\partial r^2} + \frac{1}{r}\frac{\partial \psi}{\partial r} + \frac{1}{r^2}\frac{\partial^2 \psi}{\partial \theta^2} = \frac{\partial T}{\partial r}\sin\theta + \frac{\cos\theta}{r}\frac{\partial T}{\partial \theta}, \tag{4}$$

$$\frac{\partial^2 T}{\partial r^2} + \frac{1}{r}\frac{\partial T}{\partial r} + \frac{1}{r^2}\frac{\partial^2 T}{\partial \theta^2} = -\frac{Ra}{r}\left(\frac{\partial \psi}{\partial r}\frac{\partial T}{\partial \theta} - \frac{\partial \psi}{\partial \theta}\frac{\partial T}{\partial r}\right), \tag{5}$$

where

$$u = \frac{1}{r}\frac{\partial \psi}{\partial \theta}, \quad v = -\frac{\partial \psi}{\partial r}. \tag{6}$$

If the symmetry condition at $\theta = \pi$ is enforced then (4) and (5) have to be solved subject to the boundary conditions

$$\psi = 0, \quad T = 1 \quad \text{on } r = 1, \quad 0 \leqslant \theta \leqslant \pi, \tag{7a}$$

$$u, v, T \to 0 \quad \text{as } r \to \infty, \quad 0 \leqslant \theta \leqslant \pi, \tag{7b}$$

$$\psi = \frac{\partial T}{\partial \theta} = 0 \quad \text{on } \theta = 0, \pi, \quad 1 \leqslant r < \infty. \tag{7c}$$

In order to perform calculations in a finite domain, rather than an infinite one where the location of the outer boundary condition needs careful adjustment, we employ the transformation

$$X = \frac{1}{r}. \tag{8}$$

Unfortunately this transformation leads to the stream function becoming infinite at $X = 0$ since although u and v might tend to zero as $r \to \infty$, i.e. $X \to 0$, this does not imply that the stream function likewise tends to zero. In the plume that rises above the cylinder Wooding (1963) has produced the solution for the dimensional stream function $\tilde{\psi}$ and temperature $\tilde{T}$ as follows:

$$\tilde{\psi} = \alpha (Ra_{\tilde{x}})^{\frac{1}{5}} B \tanh\left(\tfrac{1}{6} B \tilde{\eta}\right), \tag{9a}$$

$$\tilde{T} - T_\infty = \frac{\tilde{Q}}{\rho_0 c_p \alpha} (Ra_{\tilde{x}})^{-\frac{1}{5}} \tfrac{1}{6} B^2 \operatorname{sech}^2\left(\tfrac{1}{6} B \tilde{\eta}\right), \tag{9b}$$

where

$$\tilde{\eta} = (Ra_{\tilde{x}})^{\frac{1}{5}} \frac{\tilde{y}}{\tilde{x}} \tag{9c}$$

and $B = (\frac{2}{5})^{\frac{1}{5}}$. $\tilde{Q}$ is the prescribed heat flux per unit length, c_p is the specific heat of the convective fluid at constant pressure, $\tilde{x}$ and $\tilde{y}$ are the coordinates along and normal to the plume respectively, and $Ra_{\tilde{x}} = \kappa g \beta \tilde{Q} x / \alpha^2 \mu c_p$.

From (9a, b) we conclude that within the plume

$$T \sim r^{\frac{1}{5}}, \quad \psi \sim r^{\frac{1}{5}} \quad \text{as } r \to \infty \tag{10}$$

and clearly these will represent the least rapid decays in these quantities for all values of θ. This leads us to write

$$\left.\begin{aligned} &\psi = r^{\frac{4}{5}} f(r, \theta), \qquad T = r^{\frac{3}{5}} g(r, \theta) \\ \text{or} \quad &\psi = X^{-\frac{4}{5}} F(X, \theta), \quad T = X^{-\frac{3}{5}} G(X, \theta) \end{aligned}\right\} \tag{11a}$$

so that

$$F \sim X, \quad T \sim X \quad \text{as } X \to 0 \tag{11b}$$

and therefore the infinity boundary condition is easy to implement.

Substitution of the transformations (8) and (11) into (4) and (5) gives

$$X^2 \frac{\partial^2 F}{\partial X^2} - \tfrac{5}{3} X \frac{\partial F}{\partial X} + \tfrac{16}{9} F + \frac{\partial^2 F}{\partial \theta^2} = X^{-\frac{1}{5}} \left[\cos\theta \frac{\partial G}{\partial \theta} - \left(X \frac{\partial G}{\partial X} - \tfrac{2}{3} G \right) \sin\theta \right] \tag{12}$$

$$X^2 \frac{\partial^2 G}{\partial X^2} - \tfrac{1}{3} X \frac{\partial G}{\partial X} + \tfrac{4}{9} G + \frac{\partial^2 G}{\partial \theta^2} = -Ra X^{-\frac{1}{5}} \left[\frac{\partial F}{\partial \theta} \left(\frac{\partial G}{\partial X} - \frac{2}{3} \frac{G}{X} \right) - \frac{\partial G}{\partial \theta} \left(\frac{\partial F}{\partial X} - \frac{4}{3} \frac{F}{X} \right) \right] \tag{13}$$

and boundary conditions (7) become

$$\left.\begin{aligned} &F = 0, \quad G = 1, \quad X = 1, \quad 0 \leqslant \theta \leqslant \pi, \\ &F, G \to 0, \qquad\quad X \to 0, \quad 0 \leqslant \theta \leqslant \pi, \\ &F = \frac{\partial G}{\partial \theta} = 0 \quad \text{on } \theta = 0, \pi, \quad 0 \leqslant X \leqslant 1. \end{aligned}\right\} \tag{14}$$

3. Small-Rayleigh-number solution

For small values of the Rayleigh number, a solution of (4) and (5) maybe attempted by expanding the dependent variables in a series in powers, or fractional powers, of

the Rayleigh number. For the first approximation to the temperature distribution, this leads to the conduction equation

$$\nabla^2 T_0 = 0, \tag{15}$$

with the boundary conditions

$$\left.\begin{aligned} T_0 &= 1 \quad \text{on } r = 1, \quad \text{all } \theta, \\ T_0 &\to 0 \quad \text{as } r \to \infty, \quad \text{all } \theta, \\ \frac{\partial T}{\partial \theta} &= 0 \quad \text{for } r \geqslant 1, \quad \theta = 0, \pi. \end{aligned}\right\} \tag{16}$$

It is clear that (15) does not possess a solution that satisfies the boundary conditions (16). This problem was encountered by both Mahony (1957) and Fendell (1968) when considering the natural convection about an isothermally heated sphere at small Grashof numbers in a non-porous medium.

The solution of (15) that is valid in the vicinity of the cylinder and hence satisfies the boundary condition on the cylinder and a heat transfer rate corresponding to a Nusselt number Nu is

$$T_0 = 1 - Nu \ln (r). \tag{17}$$

Mahony (1957) in his study noted the futility of obtaining an exact solution for the outer region and we also came to the same conclusion for this problem. Instead a patching procedure will be followed. We seek a similarity solution of the governing equations by assuming the existence of a vertical plume and patch the temperature of the plume with that of the inner thermal field at a particular point along the x-axis.

It is found that within the plume

$$\tilde{u} = x^{-\frac{1}{3}} \tilde{f}'(\zeta), \quad T = x^{-\frac{1}{3}} \tilde{g}(\zeta), \quad \zeta = x^{-\frac{2}{3}} y, \tag{18}$$

where $\tilde{u}$ is the non-dimensional velocity component along the x-axis and x and y have been non-dimensionalized with respect to a. The governing equations then reduce to

$$\tilde{f}' = Ra\tilde{g}, \quad \tilde{g}' + \tfrac{1}{3}\tilde{f}\tilde{g} = 0, \tag{19}$$

and the boundary conditions become

$$\left.\begin{aligned} \tilde{f}(0) &= 0, \\ \tilde{f}'(\zeta), \quad \tilde{g}(\zeta) &\to 0 \quad \text{as } \zeta \to \infty, \end{aligned}\right\} \tag{20}$$

$$\int_0^\infty \tilde{f}' \tilde{g} \, \mathrm{d}\zeta = 2\pi Nu. \tag{21}$$

The solution of (19) will then define a value $\tilde{g}_0$ of $\tilde{g}$ for $\zeta = 0$. By making use of the transformation

$$\left.\begin{aligned} \tilde{f} &= Ra^{\frac{1}{3}} (3g_0)^{\frac{1}{3}} \bar{F}(\xi), \quad \tilde{g} = \tilde{g}_0 G(\xi), \\ \xi &= (Ra)^{\frac{1}{3}} (\tfrac{1}{3}\tilde{g}_0)^{\frac{1}{3}} \zeta \end{aligned}\right\} \tag{22}$$

(19) becomes

$$\bar{F}' = \bar{G}, \quad \bar{G}' + \bar{F}\bar{G} = 0, \tag{23}$$

which can be written

$$\bar{F}''' + \bar{F}\bar{F}'' = 0. \tag{24}$$

Equation (24) has to be solved subject to the boundary conditions (20), which can be written

$$\bar{F}(0) = 0, \quad \bar{F}'(0) = 1, \quad F' \to 0 \quad \text{as } \xi \to \infty. \tag{25}$$

The solution is therefore given by

$$\bar{F}(\xi) = \sqrt{2}\tanh\left(\frac{\xi}{\sqrt{2}}\right). \tag{26}$$

In order to satisfy condition (21) we must have

$$Nu\, g_0^{-\frac{3}{2}} = (Ra)^{\frac{1}{2}}\lambda, \tag{27}$$

where

$$\lambda = \frac{\sqrt{3}}{2\pi}\int_0^\infty \bar{F}'\bar{G}\,\mathrm{d}\xi. \tag{28}$$

Thus on the axis vertically above the cylinder, $\theta = \pi$, the temperature distribution is given by

$$\left.\begin{aligned} T_\ell &= g_0 x^{-\frac{1}{3}} \quad \text{at large distances from the cylinder,} \\ T_n &= 1 - Nu\ln(x) \quad \text{near the cylinder.} \end{aligned}\right\} \tag{29}$$

The necessary conditions that these solutions should join smoothly at some point x_0 are

$$\left.\begin{aligned} g_0 x_0^{-\frac{1}{3}} &= 1 - Nu\ln(x_0), \\ \tfrac{1}{3} g_0 x_0^{-\frac{4}{3}} &= x_0^{-1} Nu, \\ Nu\, g_0^{-\frac{3}{2}} &= (Ra)^{\frac{1}{2}}\lambda. \end{aligned}\right\} \tag{30}$$

From (30) we see that

$$(3 + \ln(x_0))\, Nu = 1, \tag{31}$$

which can be written

$$Nu = \tfrac{1}{3}(1 - \ln y_0)^{-1}, \tag{32}$$

where $x_0 = y_0^{-3}$. Eliminating Nu and g_0 from (30) and (32) gives

$$y_0^3(1 - \log y_0) = (3\lambda)^2 Ra. \tag{33}$$

The smallest root, y_0, of this transidental equation gives the matching point of the two solutions given in (29) and the temperature at that point is given by

$$T(x_0) = \frac{1}{(1 - \ln y_0)}. \tag{34}$$

When the Rayleigh number is very small we therefore conclude that

$$Nu \approx \frac{-1}{\ln(Ra)}, \quad x_0 \sim Ra^{-1}, \tag{35}$$

and using (32) gives

$$Nu \approx -\frac{1}{\ln(Ra)}. \tag{36}$$

The temperature distribution in the inner region can now be obtained from (29) and (36) and is given by

$$T \sim 1 + \frac{\ln(r)}{\ln(Ra)}, \quad r \text{ fixed}, \quad Ra \to 0. \tag{37}$$

Although this expression is based upon pure conduction in the inner region (as is evidenced by $\ln(r)$), the Ra-dependent coefficient indicates that the inner temperature distribution is still dependent upon thermal convection. It should be noted that this simple method of joining two solutions makes it highly unlikely that the constants in these asymptotic forms are accurately determined. However it does seem reason-

able to suppose that the functional dependence on the Rayleigh number is of the correct form.

4. Second-order boundary-layer solution

It is now convenient to write

$$r = 1+n, \quad \epsilon = (Ra)^{-\frac{1}{2}} \tag{38}$$

where n is the non-dimensional radial distance from the surface of the cylinder. Then (1), (2) and (3) can be written on eliminating the pressure as

$$\frac{\partial u}{\partial \theta}+\frac{\partial}{\partial n}[(1+n)v] = 0, \tag{39}$$

$$\frac{u}{1+n}+\frac{\partial u}{\partial n}-\frac{1}{1+n}\frac{\partial v}{\partial \theta} = \frac{\partial T}{\partial n}\sin\theta+\frac{1}{1+n}\frac{\partial T}{\partial \theta}\cos\theta, \tag{40}$$

$$\frac{1}{1+n}u\frac{\partial T}{\partial \theta}+v\frac{\partial T}{\partial n} = \epsilon^2\left\{\frac{\partial^2 T}{\partial n^2}+\frac{1}{1+n}\frac{\partial T}{\partial n}+\frac{1}{(1+n)^2}\frac{\partial^2 T}{\partial \theta^2}\right\}. \tag{41}$$

The outer expansion of the solution at high Rayleigh number is

$$\left.\begin{aligned} u &= U_1+\epsilon U_2+\ldots,\\ v &= V_1+\epsilon V_2+\ldots,\\ T &= T_1+\epsilon T_2+\ldots,\\ \psi &= \Psi_1+\epsilon \Psi_2+\ldots. \end{aligned}\right\} \tag{42}$$

Substituting (42) into (39), (40) and (41) gives, on collecting like powers in ϵ,

$$\left.\begin{aligned} &\frac{\partial U_1}{\partial \theta}+\frac{\partial}{\partial n}[(1+n)V_1] = 0,\\ &\frac{U_1}{1+n}+\frac{\partial U_1}{\partial n}-\frac{1}{1+n}\frac{\partial V_1}{\partial \theta} = \frac{\partial T_1}{\partial n}\sin\theta+\frac{1}{1+n}\frac{\partial T_1}{\partial \theta}\cos\theta,\\ &\frac{1}{1+n}U_1\frac{\partial T_1}{\partial \theta}+V_1\frac{\partial T_1}{\partial n} = 0; \end{aligned}\right\} \tag{43}$$

$$\left.\begin{aligned} &\frac{\partial U_2}{\partial \theta}+\frac{\partial}{\partial n}[(1+n)V_2] = 0,\\ &\frac{U_2}{1+n}+\frac{\partial U_2}{\partial n}-\frac{1}{1+n}\frac{\partial V_2}{\partial n}\sin\theta = \frac{\partial T_2}{\partial n}\sin\theta+\frac{1}{1+n}\frac{\partial T_2}{\partial \theta}\cos\theta,\\ &\frac{1}{1+n}U_1\frac{\partial T_2}{\partial \theta}+\frac{1}{1+n}U_2\frac{\partial T_1}{\partial \theta}+V_1\frac{\partial T_2}{\partial n}+V_2\frac{\partial T_2}{\partial n} = 0. \end{aligned}\right\} \tag{44}$$

Equations (43) and (44) have to be solved such that

$$T_1, U_1, V_1, T_2, U_2, V_2 \to 0 \quad \text{as } n\to\infty, \quad \text{all } \theta \tag{45}$$

and that as $n\to 0$ the solution matches with an inner solution.

For the inner expansion, or boundary-layer approximations, we define a new normal coordinate, $N = n/\epsilon$, and use the expansion

$$\left.\begin{aligned} u &= u_1 + \epsilon u_2 + \ldots, \\ v &= \epsilon v_1 + \epsilon^2 v_2 + \ldots, \\ T &= t_1 + \epsilon t_2 + \ldots, \\ \psi &= \epsilon \psi_1 + \epsilon^2 \psi_2 + \ldots. \end{aligned}\right\} \tag{46}$$

Substituting (46) into (39), (40) and (41) gives

$$\left.\begin{aligned} \frac{\partial u_1}{\partial \theta} + \frac{\partial v_1}{\partial N} &= 0, \\ \frac{\partial u_1}{\partial N} &= \frac{\partial t_1}{\partial N} \sin\theta, \\ u_1 \frac{\partial t_1}{\partial \theta} + v_1 \frac{\partial t_1}{\partial N} &= \frac{\partial^2 t_1}{\partial N^2}; \end{aligned}\right\} \tag{47}$$

$$\left.\begin{aligned} \frac{\partial u_2}{\partial \theta} + \frac{\partial}{\partial N}(v_2 + N v_1) &= 0, \\ u_1 + \frac{\partial u_2}{\partial N} &= \sin\theta + \frac{\partial t_1}{\partial \theta} \cos\theta, \\ u_1 \frac{\partial t_2}{\partial \theta} + u_2 \frac{\partial t_1}{\partial \theta} + v_1 \frac{\partial t_2}{\partial N} + v_2 \frac{\partial t_1}{\partial N} &= \frac{\partial^2 t_2}{\partial N^2} + N u_1 \frac{\partial t_1}{\partial N} + \frac{\partial t_1}{\partial N}. \end{aligned}\right\} \tag{48}$$

We observe that (47) has the same form as the planar boundary-layer equations for a circular cylinder embedded in a porous medium, see Merkin (1979). The second-order boundary-layer equations (48) include extra terms which take the curvature effects into consideration. Equations (47) and (48) have to be solved subject to the conditions that

$$v_1 = 0, \quad t_1 = 1, \quad v_2 = 0, \quad t_2 = 0, \quad \text{on } N = 0, \quad \text{all } \theta, \tag{49}$$

and that u, v and t match the flow variables U, V and T in an intermediate region.

Since the velocity and temperature are zero at infinity this suggests

$$U_1 = V_1 = T_1 \equiv 0, \tag{50}$$

and (47) has then to be solved subject to the boundary conditions

$$\left.\begin{aligned} v_1 = 0, t_1 = 1 \quad &\text{on } N = 0, \quad \text{all } \theta, \\ u_1, t_1 \to 0 \quad &\text{as } N \to \infty, \quad \text{all } \theta. \end{aligned}\right\} \tag{51}$$

The solution to this classical boundary-layer problem was given by Merkin (1979) using the similarity transformation

$$\left.\begin{aligned} \psi_1(\theta, N) &= 2 \sin(\tfrac{1}{2}\theta) f_1(\eta), \\ t_1(\theta, N) &= t_1(\eta), \\ \eta &= N \cos(\tfrac{1}{2}\theta), \end{aligned}\right\} \tag{52}$$

where $f_1' = t_1$ is defined by the differential equation

$$f_1''' + f_1 f_1'' = 0 \tag{53a}$$

which has to be solved subject to the boundary conditions

$$f_1(0) = 0, \quad f_1'(0) = 1, \quad f_1'(\eta) \to 0 \quad \text{as } \eta \to \infty. \tag{53b}$$

Ackroyd (1967) solved this problem and found that $f_1(\infty) = 1.14277$ and $f_1''(0) = -0.62756$ which results in the local Nusselt number ($Nu_1 = qa/(k(t_w - T_\infty))$, where k is the stagnant thermal conductivity of the saturated porous medium and q the local surface heat flux) being given by

$$Nu_1 = Ra^{\frac{1}{2}}[-f_1''(0)] \cos(\tfrac{1}{2}\theta). \tag{54}$$

The second-order outer equations (44) require to be solved subject to the appropriate matching conditions as determined by the solution (52). Since $T_2 \to 0$ as $n \to 0$ and $n \to \infty$ we conclude that T_2 is identically zero. In order to solve for the velocities we introduce the stream function such that the continuity equation is satisfied, namely

$$U_2 = \frac{\partial \Psi_2}{\partial n}, \quad V_2 = -\frac{1}{1+n}\frac{\partial \Psi_2}{\partial \theta}, \tag{55}$$

and Ψ_2 satisfies Laplace's equation

$$\frac{\partial^2 \Psi_2}{\partial n^2} + \frac{1}{1+n}\frac{\partial \Psi_2}{\partial n} + \frac{1}{(1+n)^2}\frac{\partial^2 \Psi_2}{\partial \theta^2} = 0 \quad \text{for } n > 0, \tag{56}$$

and the matching condition with the inner solution leads to

$$\Psi_2 = 2f_1(\infty) \sin(\tfrac{1}{2}\theta) \quad \text{on } n = 0. \tag{57}$$

In this second-order outer solution no mention has yet been made of the boundary conditions in θ. Clearly the solution must be symmetrical about $\theta = 0$, and $\theta = 0$ is a streamline on which $\Psi_2 = 0$ (and T_2 will also be identically zero on this line). However on the axis $\theta = \pi$ a plume will develop. At the edge of the plume the temperature will be zero and hence the conclusion that $T_2 \equiv 0$ certainly satisfies all the boundary conditions. However the stream function will have a non-zero value at the outer edge of the plume and it is clear from the solution (9) that

$$\tilde{\psi} \to \alpha (Ra_{\tilde{x}})^{\frac{1}{2}} B, \tag{58}$$

where $\tilde{x}$ is measured from some origin on the axis $\theta = \pi$. Now the heat flux $\hat{Q}$, which is a factor in the parameter $Ra_{\tilde{x}}$, is that generated on the surface of the cylinder. Therefore

$$\hat{Q} = 2c_p \rho_\infty \int_{r=1}^{\infty} \left\{ \frac{\partial \tilde{\psi}}{\partial r} (\tilde{T} - T_\infty) \right\}_{\theta = \pi} \mathrm{d}r, \tag{59}$$

where the factor 2 arises because of the contribution from the two boundary layers which originate from the generator of the cylinder at $\theta = 0$. On using the boundary-layer solution (52) we find that

$$\hat{Q} = 4\rho_\infty c_p (T_w - T_\infty) Ra_{\tilde{x}}^{\frac{1}{2}} \int_0^\infty f_1' t_1 \, \mathrm{d}\eta. \tag{60}$$

Substitution of (60) into (58) gives

$$\tilde{\psi} \to \alpha Ra^{\frac{1}{2}} 4^{\frac{1}{2}} (-f_0'')^{\frac{1}{2}} B \left(\frac{\tilde{x}}{a}\right)^{\frac{1}{2}}. \tag{61}$$

In order to find the origin of the plume solution we patch the plume solution to the boundary-layer solution (52) by enforcing that on $\theta = \pi$, $r = 1$ the stream function is continuous. If this corresponds to $x = x_0$ then equating (52) and (61) leads to

$$x_0 = 1.0569a. \tag{62}$$

Clearly there is a collision region near the generator of the cylinder at $\theta = \pi$ where we have not obtained an accurate description of the flow. We must therefore solve the Laplace's equation (56) subject to the boundary conditions

$$\left.\begin{aligned} &\Psi_2 = 2f_1(\infty)\sin(\tfrac{1}{2}\theta) && \text{on } n = 0, && 0 \leqslant \theta \leqslant \pi, \\ &\Psi_2 = 0, && \theta = 0, && 0 \leqslant n < \infty, \\ &\Psi_2 = 2.24376\,(1.0569+n)^{\frac{1}{3}}, && \theta = \pi, && 0 \leqslant n < \infty, \\ &\frac{\partial \Psi_2}{\partial n} \to 0 && \text{as } n \to \infty, && 0 \leqslant \theta \leqslant \pi, \end{aligned}\right\} \tag{63}$$

Since the second-order stream function tends to infinity as n tends to infinity we again make the following transformation

$$X = \frac{1}{1+n}, \quad \Psi_2 = X^{-\frac{4}{3}} H(X, \theta). \tag{64}$$

Equation (56) becomes

$$X^2 \frac{\partial^2 H}{\partial X^2} - \frac{5}{3} X \frac{\partial H}{\partial X} + \frac{16}{9} H + \frac{\partial^2 H}{\partial \theta^2} = 0 \tag{65}$$

and boundary conditions (63),

$$\left.\begin{aligned} &H = 2f_1(\infty)\sin(\tfrac{1}{2}\theta) && \text{on } X = 1, && 0 \leqslant \theta \leqslant \pi, \\ &H = 0 && \text{on } X = 0, && 0 \leqslant \theta \leqslant \pi, \\ &H = 0 && \text{on } \theta = 0, && 0 \leqslant X \leqslant 1, \\ &H = 2.24376X(1+0.0569X)^{\frac{1}{3}} && \text{on } \theta = \pi, && 0 \leqslant X \leqslant 1. \end{aligned}\right\} \tag{66}$$

The partial differential equation (65) was solved subject to the boundary conditions (66) using central differences with a square mesh using 10, 20, 40 and 80 subdivisions and h^2 extrapolation of the results implemented.

In order to solve for the second-order inner boundary-layer equations (48) we introduce the stream function ψ_2 such that

$$u_2 = \frac{\partial \psi_2}{\partial N}, \quad v_2 + N v_1 = -\frac{\partial \psi_2}{\partial \theta} \tag{67}$$

or in terms of the first-order inner boundary-layer variable η

$$\left.\begin{aligned} u_2 &= \cos(\tfrac{1}{2}\theta)\frac{\partial \psi_2}{\partial \eta}, \\ v_2 &= \eta\,(f_1 - \eta \tan^2(\tfrac{1}{2}\theta) f_1') - \frac{\partial \psi_2}{\partial \theta} + \tfrac{1}{2}\eta \tan(\tfrac{1}{2}\theta)\frac{\partial \psi_2}{\partial \eta}. \end{aligned}\right\} \tag{68}$$

On making these substitutions into (48) we obtain

$$\frac{\partial^2 \psi_2}{\partial \eta^2} = 2\sin(\tfrac{1}{2}\theta)\frac{\partial t_2}{\partial \eta} - 2\tan(\tfrac{1}{2}\theta) f_1' - \tfrac{1}{2}\eta \frac{\cos\theta \tan(\tfrac{1}{2}\theta)}{\cos^2(\tfrac{1}{2}\theta)} f_1'', \tag{69}$$

$$\frac{\partial^2 t_2}{\partial \eta^2} + f_1 \frac{\partial t_2}{\partial \eta} - 2\tan(\tfrac{1}{2}\theta) f_1' \frac{\partial t_2}{\partial \theta} = \left(-1 + \eta f_1 - \frac{\partial \psi_2}{\partial \theta}\right) \frac{f_1''}{\cos(\tfrac{1}{2}\theta)}, \tag{70}$$

with the boundary conditions

$$\left.\begin{aligned} \psi_2 = t_2 = 0 \quad &\text{at } \eta = 0, \qquad \text{all } \theta, \\ \frac{\partial \psi_2}{\partial \eta} \to \frac{U_2(\theta, 0)}{\cos(\tfrac{1}{2}\theta)}, \quad t_2 \to 0 \quad &\text{as } \eta \to \infty, \quad \text{all } \theta, \end{aligned}\right\} \tag{71}$$

where $U_2(\theta, 0)$ has been obtained numerically from solving the differential equation (65) subject to the boundary conditions (66).

In order to start the numerical calculations of (69) and (70) we require the starting solution at $\theta = 0$. For this we write

$$\left.\begin{aligned} \psi_2 &= \theta l(\eta) + O(\theta^2), \\ t_2 &= m(\eta) + O(\theta), \end{aligned}\right\} \tag{72}$$

and substitute into (69) retaining only leading-order terms. This gives

$$\left.\begin{aligned} l'' &= m' - f_1' - \tfrac{1}{4}\eta f_1'' \\ m'' + f_1 m' &= (-1 + \eta f_1 - l) f_1'', \end{aligned}\right\} \tag{73}$$

which have to be solved numerically subject to the boundary conditions as determined from (71).

Starting from the solution given in (73) a standard marching procedure was employed in order to solve the coupled parabolic partial differential equations (69) and (70) subject to the boundary conditions (71).

5. Finite-Rayleigh-number solution

In order to solve the partial differential equations (12) and (13) subject to the boundary conditions (14) for finite values of the Rayleigh number a finite-difference scheme is employed. A grid system is set up in the region $0 \leqslant X \leqslant 1$ and $0 \leqslant \theta \leqslant \pi$. Constant radial and angular mesh sizes $h = 1/M$ and $k = \pi/N$ are used, where M and N are integers. We denote all quantities at a typical set of grid points (X_0, θ_0), $(X_0, \theta_0 + k)$, $(X_0 + h, \theta_0)$, $(X_0, \theta_0 - k)$ and $(X_0 - h, \theta_0)$ by the subscripts 0, 1, 2, 3 and 4 respectively. Replacing (12) and (13) by central differences everywhere results in a set of finite-difference equations which may have associated matrices that are not diagonally dominant. If this occurs then it will do so in only a limited region of the computational domain and for large values of the Rayleigh number. It must be remembered that diagonal dominance is a sufficient condition for convergence of the Gauss–Seidel iterative procedure, and also for the successive over-relaxation procedure for a well-defined range of the relaxation parameter, but not a necessary condition. However if a scheme can be devised in which the associated matrices are diagonally dominant then this would ensure convergence. The matrices associated with the finite-difference equations obtained by using central differences for the second-order derivatives and forward or backward differencing of the first-order derivatives depending on the direction of the flow gives rise to matrices which are

diagonally dominant, but a big disadvantage of this method is that the error in the finite-difference equations is first order.

Allen & Southwell (1955) developed a method of representing the two-dimensional Navier–Stokes equations in finite-difference form in which the associated matrices are diagonally dominant and the truncation error is only of second order. These and related methods have been extended by several authors, e.g. Dennis & Hudson (1978), Dennis *et al.* (1979), to deal with the Navier–Stokes equations in Cartesian coordinates. In this paper we extend these methods in order to deal with (13) as the solution of (12) for F causes no difficulties for a given G. We therefore write (13) in the form

$$X^2\frac{\partial^2 G}{\partial X^2}-\tfrac{1}{3}X\frac{\partial G}{\partial X}+X^2 p\frac{\partial G}{\partial X}-\tfrac{2}{3}Ra\,X^{-\frac{4}{3}}G+\tfrac{4}{9}G+\frac{\partial^2 G}{\partial\theta^2}+q\frac{\partial G}{\partial\theta}=0, \tag{74}$$

where

$$p=\frac{Ra\,X^{-\frac{1}{3}}}{X^2}\frac{\partial F}{\partial\theta},\quad q=-Ra\,X^{-\frac{1}{3}}\left(\frac{\partial F}{\partial X}-\frac{4}{3}\frac{F}{X}\right), \tag{75}$$

and split (74) into two components

$$X^2\frac{\partial G}{\partial X}-\tfrac{1}{3}X\frac{\partial G}{\partial X}+pX^2\frac{\partial G}{\partial X}-G[\tfrac{2}{3}Ra\,X^{-\frac{4}{3}}-\tfrac{4}{9}]=A, \tag{76}$$

$$\frac{\partial^2 G}{\partial\theta^2}+q\frac{\partial G}{\partial\theta}=-A, \tag{77}$$

where A is an unknown function of X and θ. Equation (76) is transformed locally for $X_0-h\leqslant X\leqslant X_0+h$, $\theta=\theta_0$ by the substitution

$$G=\lambda\,\mathrm{e}^{-s},\quad s(X,\theta_0)=\frac{1}{2}\int_{X_0}^{X}p\,\mathrm{d}X, \tag{78}$$

whilst (77) is transformed locally for $X=X_0$, $\theta_0-k\leqslant\theta\leqslant\theta_0+k$ by the substitution

$$G=\nu\,\mathrm{e}^{-\tilde{s}},\quad \tilde{s}(X_0,\theta)=\frac{1}{2}\int_{\theta_0}^{\theta}q\,\mathrm{d}\theta. \tag{79}$$

Substituting the transformations (78) and (79) into (76) and (77) respectively gives

$$X^2\frac{\partial^2\lambda}{\partial X^2}-\frac{X}{3}\frac{\partial\lambda}{\partial X}+\lambda X^2\left[-\frac{1}{2}\frac{\partial p}{\partial X}+\frac{1}{6X}p-\tfrac{1}{4}p^2-\frac{1}{X^2}(\tfrac{2}{3}Ra\,X^{-\frac{4}{3}}-\tfrac{4}{9})\right]=A\,\mathrm{e}^{s}, \tag{80}$$

$$\frac{\partial^2\nu}{\partial\theta^2}+\nu\left[-\tfrac{1}{4}q^2-\frac{1}{2}\frac{\partial q}{\partial\theta}\right]=-A\,\mathrm{e}^{\tilde{s}}. \tag{81}$$

Evaluating (80) and (81) at the point (X_0,θ_0), replacing all derivatives with central differences and eliminating the unknown A_0 between these two equations gives

$$\lambda_1\left[1-\frac{h}{6X_0}\right]+\lambda_3\left[1+\frac{h}{6X_0}\right]+\frac{\gamma^2}{X_0^2}[\nu_2+\nu_4]+\lambda_0$$
$$\times\left[-4+\frac{h^2}{X_0^2}\left\{-\tfrac{1}{2}X_0^2\frac{\partial p}{\partial X}+\tfrac{1}{6}pX_0-\tfrac{1}{4}p^2X_0^2-(\tfrac{2}{3}Ra\,X_0^{-\frac{4}{3}}-\tfrac{4}{9})-\frac{q^2}{4}-\frac{1}{2}\frac{\partial q}{\partial\theta}\right\}\right]=0, \tag{82}$$

where $\gamma^2=h^2/k^2$.

The functions λ_1, λ_3, ν_2 and ν_4 involve exponential functions and we therefore use the method as described by Dennis & Hudson (1978) to eliminate these functions. The quantities s and $\tilde{s}$ are evaluated using Taylor series and then performing the

integrations and the resulting exponential function can then be expanded, giving rise to the finite-difference equation

$$G_1\left[1+\tfrac{1}{2}p_0 h-\frac{h}{6X_0}+\underline{\tfrac{1}{8}p_0^2 h^2}\right]+G_3\left[1-\tfrac{1}{2}p_0 h+\frac{h}{6X_0}+\underline{\tfrac{1}{8}p_0 h^2}\right]$$
$$+G_2\frac{\gamma^2}{X_0^2}[1+\tfrac{1}{2}q_0 k+\underline{\tfrac{1}{8}q_0^2 k^2}]+G_4\frac{\gamma^2}{X_0^2}[1-\tfrac{1}{2}q_0 k+\underline{\tfrac{1}{8}q_0^2 k^2}]$$
$$+G_0\left[-4-\underline{\frac{h^2}{4}(p_0^2+q_0^2)}-\frac{h^2}{X_0^2}(\tfrac{2}{3}Ra\,X_0^{-\frac{4}{3}}-\tfrac{4}{9})\right]=0 \tag{83}$$

where terms of second-order accuracy have been retained. The terms underlined are the second-order accuracy terms that exist in addition to what would have been obtained with a straightforward implementation of central differences.

The coefficients of the terms involving G_1 and G_3 are of the form $1+\beta+\frac{1}{2}\beta^2\pm h/6X_0$, whilst those involving the G_2 and G_4 are of the form $(\gamma^2/X_0^2)(1+\delta+\frac{1}{2}\delta^2)$. Since the minimum value of $1+\beta+\frac{1}{2}\beta^2$ for any value of β is $\frac{1}{2}$ and $X_0 \geqslant h$ then

$$\left.\begin{aligned}&\frac{\gamma^2}{X_0^2}(1+\delta+\tfrac{1}{2}\delta^2)>0,\\ \text{and}\qquad &1+\beta+\tfrac{1}{2}\beta^2\pm\frac{h}{6X_0}>\frac{1}{3}.\end{aligned}\right\} \tag{84}$$

Further $(\frac{2}{3}Ra\,X^{-\frac{4}{3}}-\frac{4}{9})$ is always positive if $Ra>\frac{2}{3}$. We therefore conclude that the matrix associated with the finite-difference equation (83) is diagonally dominant for $Ra>\frac{2}{3}$. It should however be remembered that (12) and (13) have to be solved simultaneously and although the finite-difference equations may be diagonally dominate individually the coupled system may, and probably will, not be diagonally dominant. However it would be expected that this method would make the coupled associated matrices 'nearer' to being diagonally dominant because the method tries to deal with the terms that cause the loss of diagonal dominance in the central-difference method. Thus it may be expected that when using this method then a larger relaxation parameter may be used than would have been possible without the underlined terms in (83).

The smallest value of the Rayleigh number for which numerical calculations were performed was $Ra=10^{-2}$. For this computation the unknown variables F and G were set identically to zero at all mesh points. The order of solution was as follows. Starting from this initial solution one complete Gauss–Seidel iteration was carried out over all internal grid points for G and F in that order. The iterative sweep was carried out starting at $X=h$, $\theta=k$, proceeding along all grid points at constant X, followed by all grid points at constant $X=2h$ starting at $\theta=k$, etc. The new boundary condition on G at each grid point on $\theta=0$ and $\theta=\pi$ was then found. This whole sequence of operations is defined as one iteration. The above procedure was repeated until

$$\Sigma\left\{\left|1-\frac{F^{(m)}}{F^{(m+1)}}\right|+\left|1-\frac{G^{(m)}}{G^{(m+1)}}\right|\right\}<\epsilon, \tag{85}$$

where the summation is over all grid points, the superscripts denote the number of iterations and ϵ is an assigned tolerance for which a variation by a value of 10^{-4} was found to be sufficient. The converged solution at $Ra=10^{-2}$ was then used for the initial guess of the solution at the next value of Ra, say 10^{-1}, and these processes were repeated up to a value of $Ra=400$.

In all calculations the method of solution always produced converged results without having recourse to under-relaxation. Calculations could in fact have been speeded up by the inclusion of an over-relaxation parameter. Even though the above theory only suggests that for $Ra > \frac{2}{3}$ the matrix associated to the finite-difference equations (83) is diagonally dominant it was found that this expanded exponential method converges faster than the conventional central-difference technique for all values of Ra.

In order to check the accuracy of this method the solution corresponding to the use of central differences everywhere was obtained. This was achieved at a given Rayleigh number by using the converged expanded exponential solution as the first estimate of the solution and using a simple modification of the computational program used for the expanded exponential solution. It was found that at small values of Rayleigh numbers a straightforward Gauss–Seidel procedure may be employed but as the Rayleigh number increases an under-relaxation procedure has to be employed with an under-relaxation that may be as small as 10^{-1} for $Ra = 400$.

The expanded exponential method produced converged solutions of the finite-difference equations for values of $Ra > 400$ but the accuracy of these results must be questionable because of the lack of information within the boundary layer on the cylinder and within the wake.

6. Results and discussions

Numerical calculations were performed with $h = k/\pi = \frac{1}{10}, \frac{1}{20}, \frac{1}{40}, \frac{1}{60}$ and $\frac{1}{80}$ and for $Ra = 10^{-2}, 10^{-1}, 1, 10, 20, 40, 70, 100, 150, 200, 300$ and 400. Results were obtained for both the expanded exponential method and standard central finite differences. It was found that in both cases that h^2 extrapolation was appropriate and that for a given mesh size the standard central-difference solution was closer to the extrapolation solution than the expanded exponential solution. However the expanded exponential method does provide an easier and faster means of obtaining the converged solution to the central-difference formulation. Although it was found that numerical 'results' could be obtained for values of $Ra \gg 400$ the extrapolated solution was significantly different (of the order of 10 % or larger) from the solution on the finest grid to cause concern. This is because there were insufficient mesh points within the boundary layer and plume for the 'results' to be physically significant.

Table 1 shows the variation of the average Nusselt number, which is defined by

$$\overline{Nu} = -\frac{1}{2\pi}\int_0^{2\pi}\left(\frac{\partial T}{\partial r}\right)_{r=1} \mathrm{d}\theta = \frac{1}{\pi}\int_0^{\pi}\left(\frac{\partial G}{\partial X}\right)_{X=1} \mathrm{d}\theta - \tfrac{2}{3}, \tag{86}$$

as the function of the Rayleigh number as obtained from the numerical solution of (12) and (13). These results represent the h^2 extrapolated values from the central-difference formulation using the finest grids. For large Rayleigh numbers the boundary-layer solution given by (52) gives

$$\overline{Nu} = -\frac{1}{\pi}\int_0^{\pi} t'(0)\cos(\tfrac{1}{2}\theta)\,\mathrm{d}\theta = 0.3995 Ra^{\frac{1}{2}} \tag{87}$$

and this is also tabulated in table 1. At first sight it might be thought that the discrepancy between the boundary-layer solution and the numerically obtained solution is large. However if we make the assumption that the boundary-layer result (87) can be extended in the form

$$\overline{Nu} = 0.3995 Ra^{\frac{1}{2}} + a + b\,Ra^{-\frac{1}{2}} + \ldots \tag{88}$$

Ra	Boundary-layer solution $0.3995171Ra^{\frac{1}{2}}$	$0.3995171Ra^{\frac{1}{2}}$ $+0.78-1.9Ra^{-\frac{1}{2}}$	Numerical solution
1	0.3995	−0.7125	0.491
10	1.2634	1.4426	1.578
20	1.7867	2.1418	2.183
40	2.5268	3.0064	3.008
70	3.3426	3.8955	3.888
100	3.9952	4.5852	4.582
150	4.8931	5.5179	5.528
200	5.6500	6.2957	6.322
300	6.9198	7.5901	7.603
400	7.9903	8.6753	8.691

TABLE 1. The variation of the average Nusselt number as a function of the Rayleigh number

h	$Ra = 40$	$Ra = 300$
$\frac{1}{20}$	3.122	10.058
$\frac{1}{40}$	3.036	8.118
$\frac{1}{60}$	3.020	7.818
$\frac{1}{80}$	3.015	7.724
Extrapolation	3.008	7.603

TABLE 2. The variation of the average Nusselt number as a function of mesh size for Rayleigh numbers 40 and 300

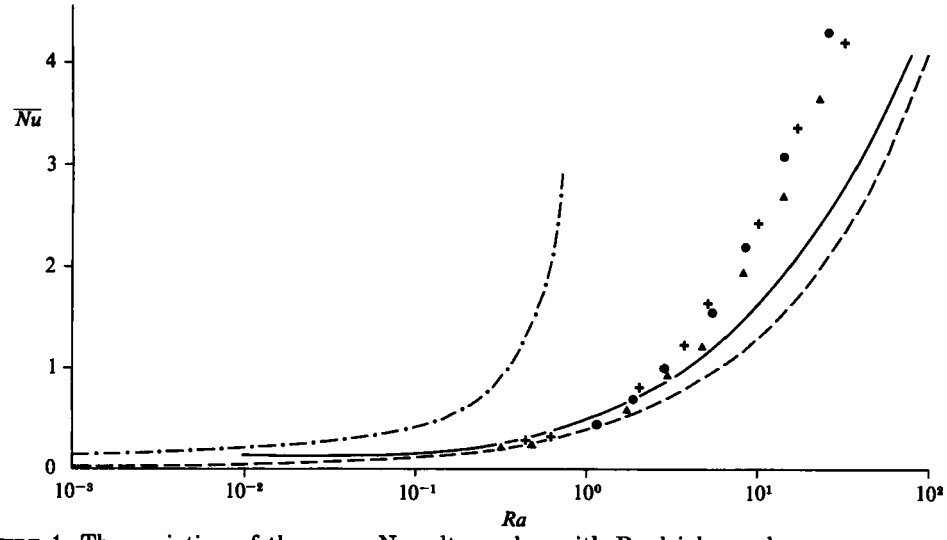

FIGURE 1. The variation of the mean Nusselt number with Rayleigh number. ——, numerical solution: – – –, boundary-layer solution; –·–·–, small-Rayleigh-number solution; ·, △, +, experimental results using spheres of diameter 2, 3 and 4 mm respectively.

then taking the empirical constants $a = 0.78$ and $b = -1.9$, the results for $\overline{Nu}$ are seen, in table 1, to give an excellent agreement with the results obtained from the numerical method.

To illustrate the extrapolation used, table 2 shows the variation of $\overline{Nu}$ using $h = k/\pi = \frac{1}{20}, \frac{1}{40}, \frac{1}{60}$ and $\frac{1}{80}$ for $Ra = 40$ and 300. Also shown are the extrapolated values

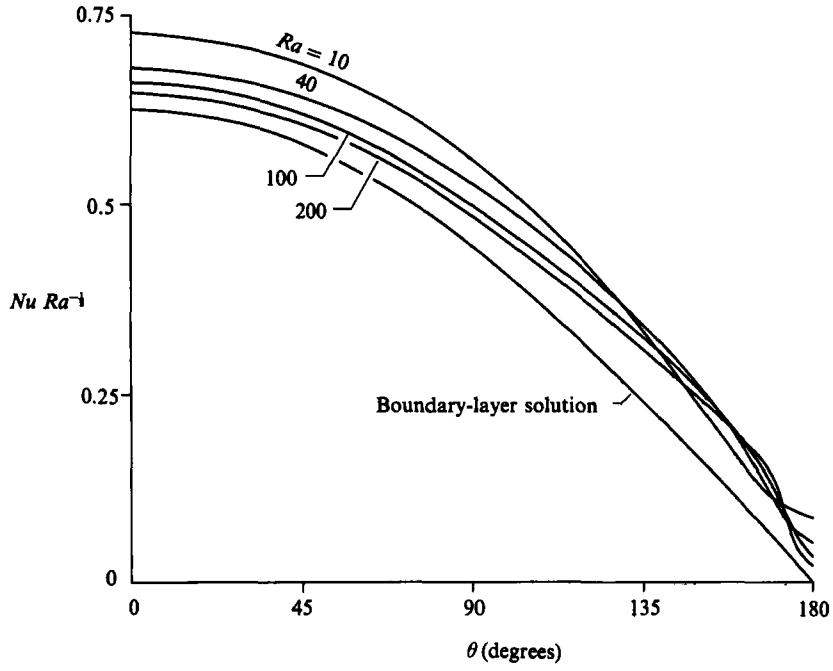

FIGURE 2. The variation of the local Nusselt number as a function of θ for various values of the Rayleigh number.

Ra	$-\left(\frac{\partial T}{\partial r}\right)_{r=1}$	$0.422-0.3Ra^{-\frac{1}{4}}$
10	0.321	0.327
20	0.353	0.355
40	0.374	0.375
70	0.386	0.386
100	0.392	0.392
150	0.398	0.398
200	0.401	0.401
300	0.405	0.405
400	0.407	0.407

TABLE 3. The variation of the Nusselt number at $\theta = 0$ as a function of the Rayleigh number

using the two finest grids and these results illustrate the accuracy to which the numerical results are being obtained. In all the following h^2 extrapolated results are presented.

The variation of the mean Nusselt number with Rayleigh number is shown in figure 1. The boundary-layer solution is presented along with the numerical solution and it is seen that the boundary-layer solution gives a reasonable approximation even for Rayleigh numbers as small as 10^{-1}. Also shown in the figure is the low-Rayleigh-number solution given by (36). It must be remembered that this solution is only valid when $-\ln(Ra) \gg 1$ and therefore its regime of validity is probably not within the range of values of Ra shown. Further, as has already been noted, the constants in the asymptotic solution have not been accurately determined and hence

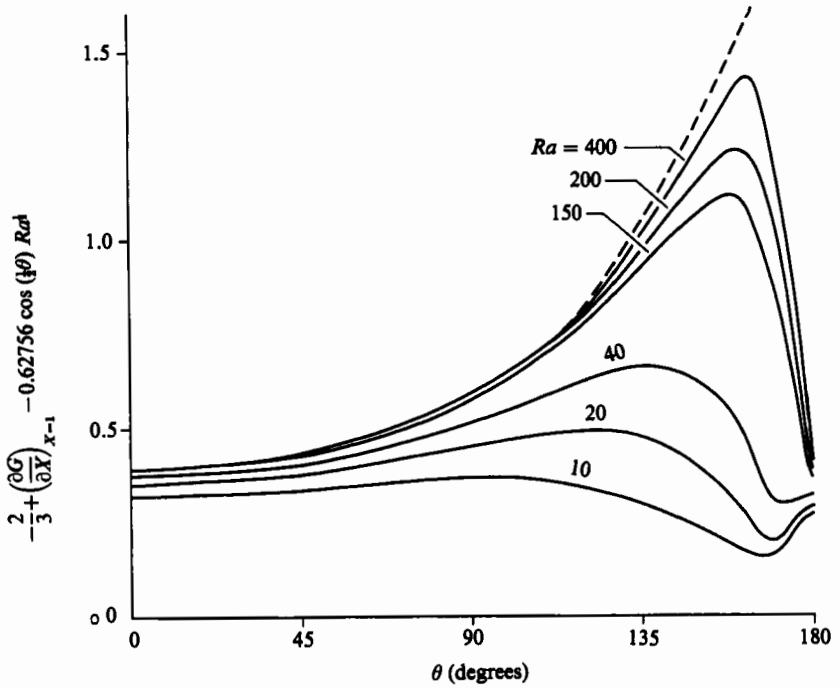

FIGURE 3. The variation of $-\frac{2}{3}+(\partial G/\partial X)_{X=1}-0.62756\cos(\frac{1}{2}\theta)\,Ra^{\frac{1}{2}}$ as a function of θ for various values of Ra. ——, limiting behaviour as $Ra\to\infty$ as predicted by the second-order boundary-layer solution.

Ra	$180°-\theta$	$79R^{-\frac{1}{2}}$	$\bar{N}u_m$	$0.32Ra^{\frac{1}{2}}$
40	43.1	31.4	0.66	0.80
70	36.4	27.3	0.81	0.93
100	26.1	25.0	0.91	1.01
150	21.7	22.6	1.09	1.12
200	20.4	21.0	1.21	1.20
300	18.5	19.0	1.34	1.33
400	17.3	17.7	1.42	1.43

TABLE 4. The variations of θ_c and $\bar{N}u_m$ with the Rayleigh number

this variation of Nusselt number with Rayleigh number only qualitatively shows the variation at small Rayleigh numbers.

Fand *et al.* (1985) have experimentally investigated the heat transfer from a horizontal cylinder embedded in a porous medium consisting of randomly packed glass spheres of radii 2, 3 and 4 mm in either water or silicone oil at 20 °C. The results for water, as presented in table 3 of Fand *et al.*, are given in figure 1. It is seen that the experimental results are in reasonable agreement with the numerical results when $Ra \lesssim 10$ but there is an increasing discrepancy as Ra increases above 10. However Fand *et al.* state that their results can be divided into two subregions, called 'low' and 'high', in each of which the Nusselt number behaves differently. In the low-Ra region the flow is Darcian whereas the high-Ra region corresponds to Forchheimer flow. Thus it must be concluded that the results of the experiments and numerical work in the low-Ra region should agree as the governing equations adequately model

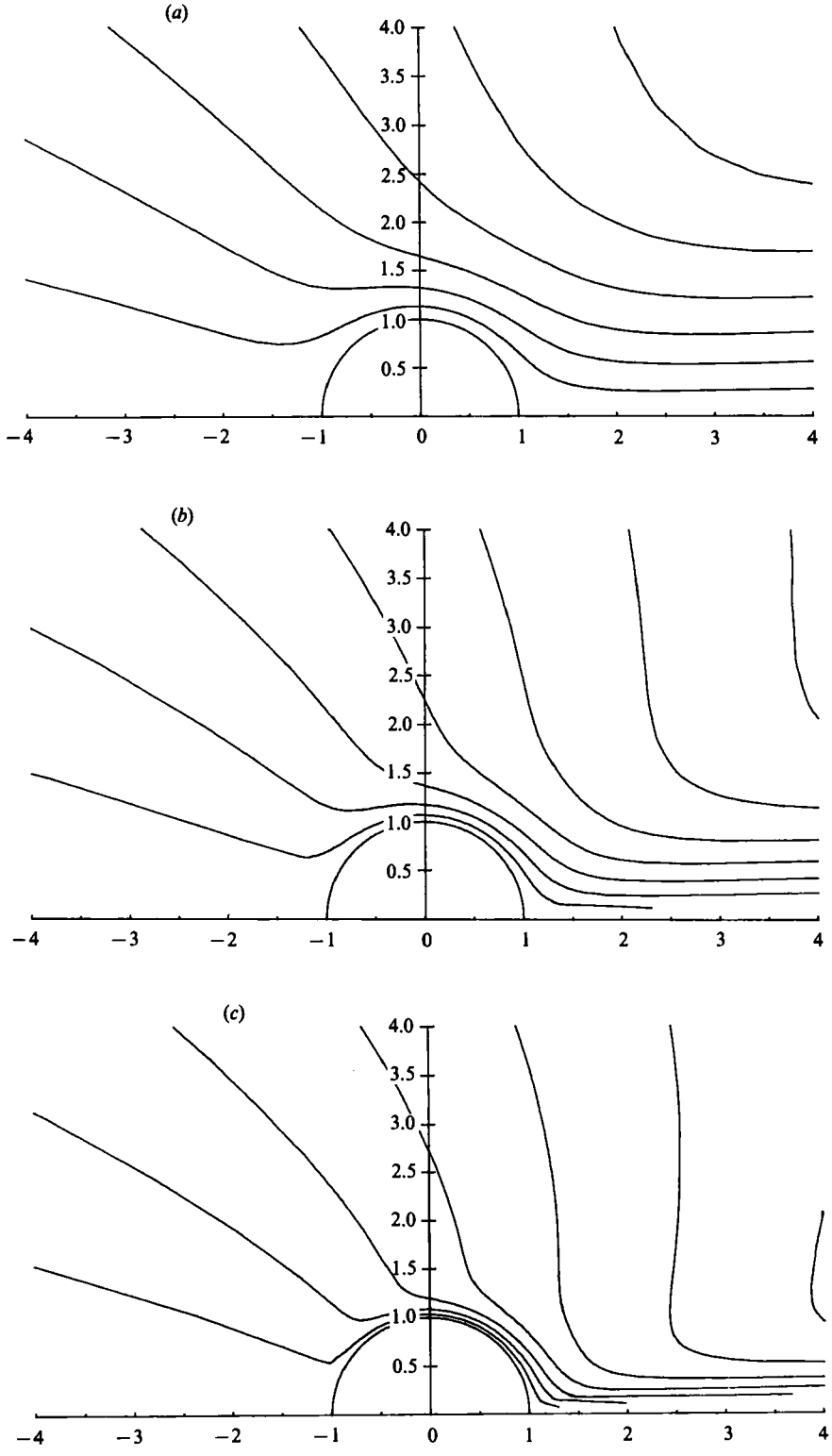

FIGURE 4 (*a–c*). For caption see facing page.

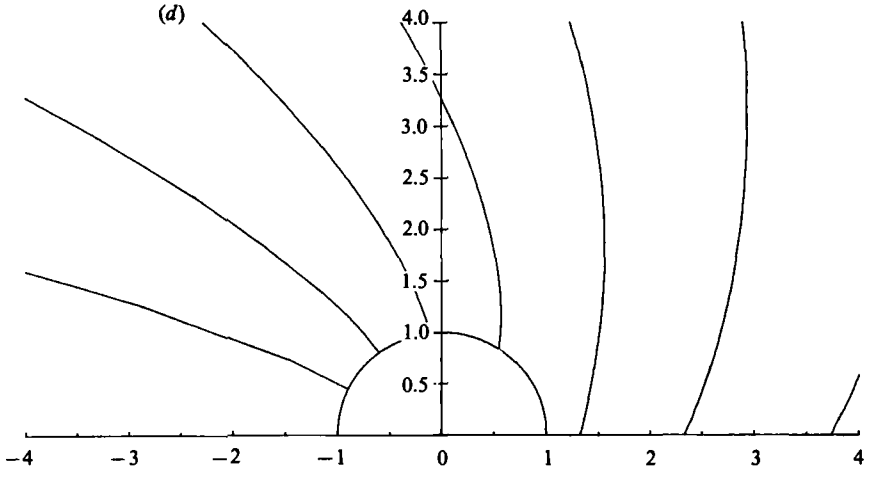

FIGURE 4. The streamlines in the vicinity of the cylinder. (*a*) $Ra = 10$, (*b*) 40, (*c*) 200, (*d*) asymptotic solution.

the flow. However in the high-Ra region when non-Darcian effects are present in the experiments it is not too surprising that the theory and experimental results disagree.

It is clear from the experimental work of Fand *et al.* (1986) that even at Rayleigh numbers as low as order 10 non-Darcian effects become important. This must therefore call into question much of the present day research that investigates the boundary-layer solutions, $Ra \gg 1$, for Darcian flow. Ingham (1987) recognizing this situation developed a theory for a non-Darcian free convection boundary layer on axisymmetric and two-dimensional bodies of arbitrary shape from which it was observed that the average Nusselt number varied as $Ra^{\frac{1}{2}}$ rather than the $Ra^{\frac{1}{4}}$ predicted by the Darcian theory as given by Merkin (1979). Fand *et al.* (1986), on the basis of experimental results for $Ra \lesssim 200$, found that the average Nusselt number varied from $Ra^{0.694}$ at low Rayleigh numbers ($\lesssim O(10)$) to $Ra^{0.372}$ for high Rayleigh numbers (but still less than 200). Thus as the Rayleigh number increases to higher values perhaps the power of the Rayleigh-number variation will reduce further towards the predicted limit of $\frac{1}{4}$. However it is clear that the discrepancy between the theory and experimental results arises because the governing model no longer adequately describes the experimental configuration. In order to apply Darcy's law the size of the pores must be much smaller than the scale of the bulk flow and inertial and thermal lengthscales.

Figure 2 shows the variation of the local Nusselt number,

$$Nu\left(=-\left(\frac{\partial T}{\partial r}\right)_{r=1}=-\frac{2}{3}+\left(\frac{\partial G}{\partial X}\right)_{X=1}\right),$$

as a function of θ for various values of the Rayleigh number. Also shown is the boundary-layer solution as predicted by Merkin (1979), $Nu = 0.62756 \cos(\frac{1}{2}\theta)\, Ra^{\frac{1}{2}}$. It is seen that as the Rayleigh number increases the general trend is quite consistent with the limiting boundary-layer solution. The approach to the boundary-layer solution being much clearer the smaller the value of θ, as one would have expected since the boundary layer emanates from $\theta = 0$.

Table 3 shows the variation of the local Nusselt number, $-(\partial T/\partial r)_{r=1}$, at $\theta = 0$ as a function of the Rayleigh number. The limiting value as $Ra \to \infty$ as obtained from

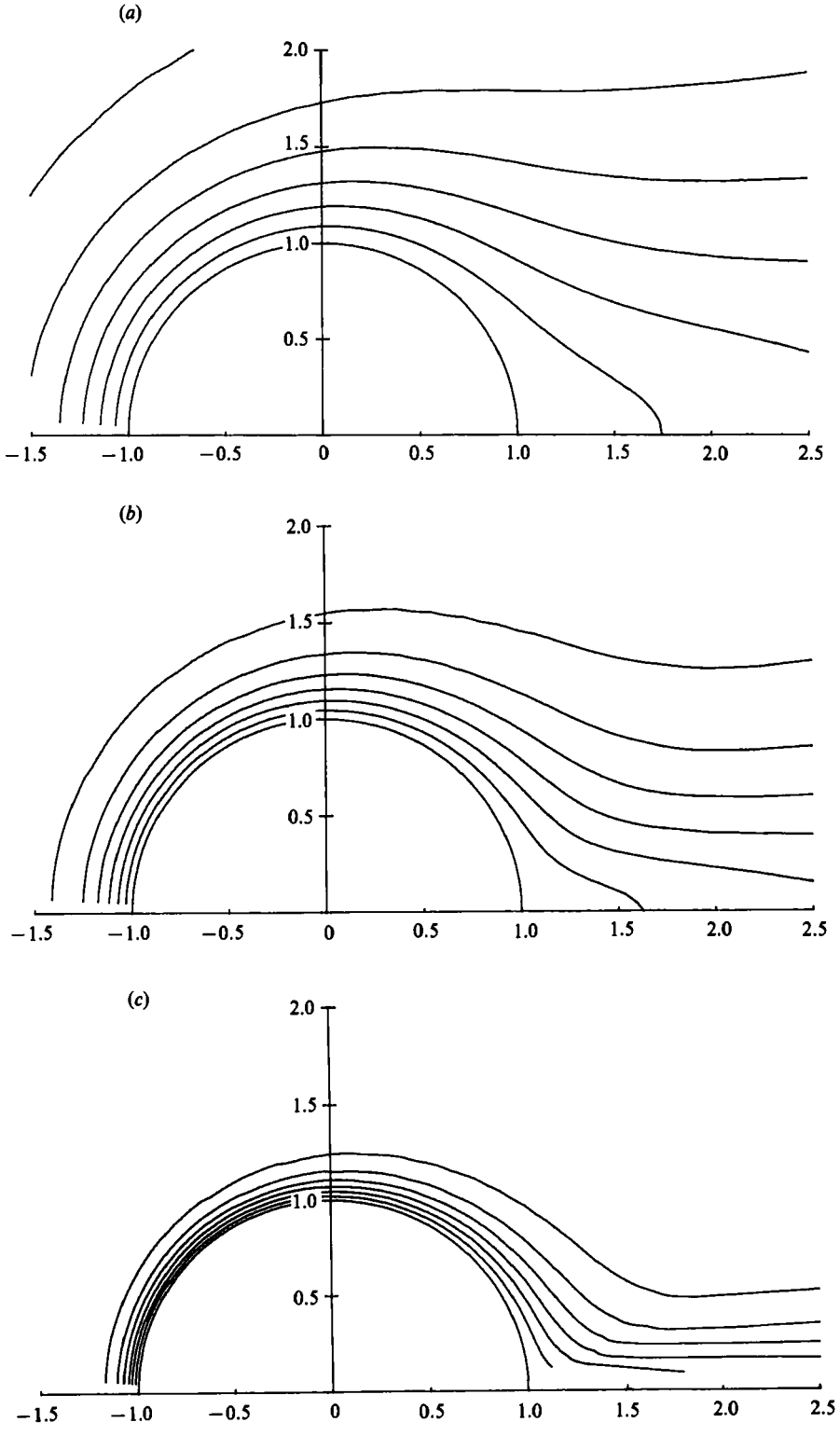

FIGURE 5. The isotherms in the vicinity of the cylinder (*a*) $Ra = 10$, (*b*) 40, (*c*) 200.

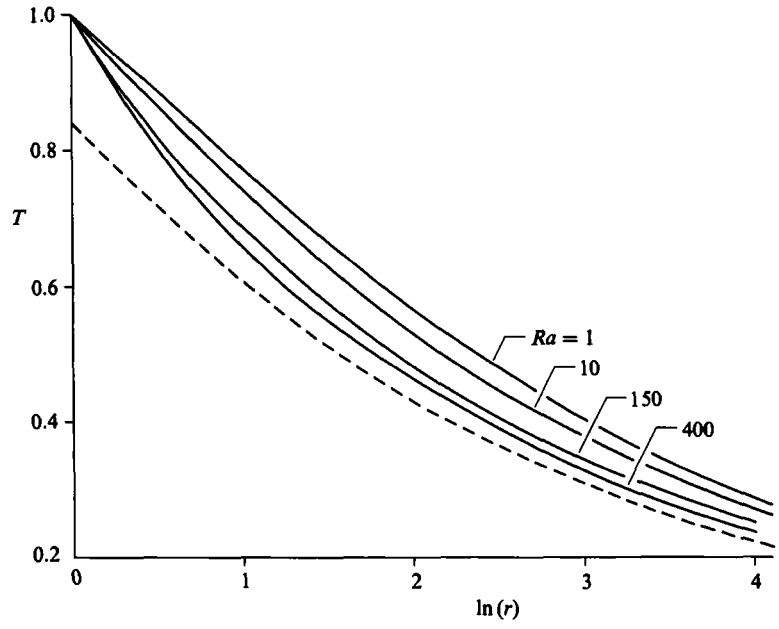

FIGURE 6. The variation of the non-dimensional temperature along the axis of the plume as a function of distance from the centre of the cylinder for various values of the Rayleigh number. ----, limiting behaviours as $Ra \to \infty$ as predicted by the boundary-layer analysis.

the second-order boundary-layer theory is 0.422 but the approach to this value is rather slow. Assuming that the correction to this value is $O(Ra^{-\frac{1}{4}})$, i.e. $-(\partial T/\partial r)_{r=1} = 0.422 + d\,Ra^{-\frac{1}{4}}$, where d is an unknown empirical constant, and if we choose $d = -0.3$, table 3 shows that this gives a good agreement with the numerically predicted values.

The behaviour of the solution near $\theta = 180°$ looks a little complex and therefore in figure 3 we plot the difference between the local Nusselt number, as obtained from the numerical calculations, and that predicted by the boundary-layer solution, i.e. $-\frac{2}{3} + (\partial G/\partial X)_{X=1} - 0.62756 \cos(\frac{1}{2}\theta)\, Ra^{\frac{1}{4}}$, for various values of the Rayleigh number. Also shown is the second-order boundary-layer correction. It is clearly seen that as the Rayleigh number is increased the second-order boundary-layer solution is being approached everywhere except near $\theta = 180°$. This discrepancy near $\theta = 180°$ is not surprising as the first-order boundary-layer solution and the plume solution were only patched in this vicinity. In fact from (69) and (70) we see that both ψ_2 and t_2 behave as $(\pi - \theta)^{-3}$ as θ tends to π.

In the theory by Smith & Duck (1977) the collision of the boundary layers is accompanied by separation of the flow to form a recirculating region of dimension $O(Ra^{-\frac{3}{4}})$. No such region exists in the calculations performed up to $Ra = 400$ and there are no indications to suggest that such a region is being approached. A measure of the size of the collision region can be taken to be the angular distance between the radii to the uppermost generator of the cylinder and the position of the maximum value of $-\frac{2}{3} + (\partial G/\partial X)_{X=1} - 0.62756 \cos(\frac{1}{2}\theta)\, Ra^{\frac{1}{4}}$, say θ_c, given in figure 3. The variation of θ_c with Ra is given in table 4 which also shows the function $C\,Ra^{-\frac{1}{4}}$, for $C = 79$. The agreement between these two functions is fairly good for this value of C. Another measure of the scales appropriate in the collision region is the maximum magnitude of $-\frac{2}{3} + (\partial G/\partial X)_{X=1} - 0.62756 \cos(\frac{1}{2}\theta)\, Ra^{\frac{1}{4}}$, say $\bar{N}u_m$ and the variation of

this with Rayleigh number is shown in table 4. Also shown in the table is the variation of $B\,Ra^{\frac{1}{4}}$ for $B = 0.32$ and the agreement between the two functions is again good.

From the scalings given by Smith & Duck (1977) we might expect $\frac{3}{14}$ powers rather than $\frac{1}{4}$ powers but the numerical calculations cannot be performed for sufficiently high values of the Rayleigh number to determine accurately these powers and the constants B and C. However the results suggest that the region of interaction of the collision of the boundary layers is reasonably consistent with the theory of Smith & Duck but no flow reversals are observed.

The streamline pattern in the vicinity of the cylinder is shown in figure 4 for various values of the Rayleigh number and the streamlines are equally spaced at intervals of $0.5Ra^{\frac{1}{2}}$. Also shown is the limiting streamline pattern as $Ra \to \infty$ as obtained from the numerical solution of the governing equation (65) subject to the boundary conditions (66). It is observed that as the Rayleigh number increases the asymptotic solution appears to be being approached and there is no evidence of a recirculating zone being developed near $r = 1$, $\theta = 180°$.

Figure 5 shows the isotherms in the vicinity of the cylinder for various values of the Rayleigh number and the lines are equally spaced at intervals of 0.15. It is observed that as the Rayleigh number increases the temperature tends to zero everywhere except in the vicinity of the cylinder and in the plume, and the width of the plume decreases as predicted.

In the wake we see from (96) that the temperature decays as $\tilde{x}^{-\frac{1}{3}}$. On using the patching of the boundary-layer solution on the cylinder and the wake solution we have already found that there is an origin shift as given by (62) and in fact the non-dimensional temperature T on the axis of the wake is predicted to be given by

$$T = 0.8391\left(\frac{1}{X} + 0.0569\right)^{-\frac{1}{3}} \tag{89}$$

from the first-order boundary-layer theory.

The variation of the non-dimensional temperature on the axis of the plume with the distance from the centre of the cylinder for various values of the Rayleigh number and the boundary-layer prediction as given by (89) is shown in figure 6. It is observed that as the Rayleigh number increases the asymptotic boundary-layer solution is being approached at large distance from the cylinder. Clearly near the cylinder the wake solution has not fully developed and the asymptotic boundary-layer solution is not appropriate.

Part of this work was done whilst one of the authors (D.B.I.) was visiting the University of Hawaii. We would like to thank Professor P. Cheng for making this visit possible and for his valuable comments on the work.

REFERENCES

Ackroyd, J. A. D. 1967 *Proc. Camb. Phil. Soc.* **63**, 871.

Allen, D. N. de G. & Southwell, R. V. 1955 *Q. J. Mech. Appl. Maths* **8**, 129.

Banks, W. H. H. 1965 *Q. J. Mech. Appl. Maths* **18**, 443.

Banks, W. H. H. 1976 *Acta Mech.* **24**, 273.

Beavers, G. S. & Sparrow, E. M. 1969 *Trans. ASME* E: *J. Appl. Mech.* **26**, 711.

Burns, P. J. & Tien, C. L. 1979 *Intl J. Heat Mass Transfer* **22**, 929.

Caltagirone, J. P. 1976 *J. Fluid Mech.* **76**, 337.

CHENG, P. 1985 In *Proc. Advanced Study Institute on Natural Convection: Fundamentals and Applications* (ed. S. Kakac, W. Aung & R. Viskanta), pp. 312–351. Hemisphere.

CHENG, P. & HSU, C. T. 1984 *Trans. ASME* C: *J. Heat Transfer* **106**, 143.

DARCY, H. 1856 *Les Fontaines Publiques de la Ville de Dijon*. Dalmont.

DENNIS, S. C. R. 1960 *Q. J. Mech. Appl. Maths* **13**, 487.

DENNIS, S. C. R. 1973 *Proc. 3rd Intl Conf. on Numerical Methods in Fluid Mechanics, vol. 2* (ed. H. Cabannes & R. Teman), Lecture Notes in Physics, vol. 19, p. 129. Springer.

DENNIS, S. C. R. & HUDSON, J. D. 1978 *Proc. Intl Conf. on Numerical Methods in Laminar and Turbulent Flow, Swansea, UK*, p. 69. London: Pentech.

DENNIS, S. C. R., INGHAM, D. B. & COOK, R. N. 1979 *J. Comp. Phys.* **33**, 325.

FAND, R. M., STEINBERGER, T. E. & CHENG, P. 1986 *Intl J. Heat Mass Transfer* **29**, 119.

FENDELL, F. E. 1968 *J. Fluid Mech.* **34**, 163.

FORCHHEIMER, P. H. 1901 *Zeitschrift des Vereines, Deutscher Ing.* **45**, 1782.

FORNBERG, B. 1980 *J. Fluid Mech.* **97**, 819.

HARDEE, H. C. 1976 *Sandia Laboratories Rep.* SAND 76-0075.

INGHAM, D. B. 1987 *Intl J. Heat Mass Transfer* (to be published).

KUEHN, T. H. & GOLDSTEIN, R. J. 1980 *Intl J. Heat Mass Transfer* **23**, 971.

MAHONY, J. J. 1957 *Proc. R. Soc. Lond.* A **238**, 412.

MERKIN, J. H. 1979 *Intl J. Heat Mass Transfer* **22**, 1461.

MUSKAT, M. 1946 *The Flow of Homogeneous Fluids Through Porous Media*. Michigan: J. W. Edwards.

NIELD, D. A. 1985 *Proc. CSIRO/DSIR Seminar on Convective Flows in Porous Media, Wellington, New Zealand*, p. 6.

NIGAM, S. D. 1954 *Z. angew Math. Phys.* **5**, 151.

ROSCOE, D. F. 1975 *J. Inst. Maths Applics* **16**, 291.

ROSCOE, D. F. 1976 *Intl J. Numer. Meth. Engng* **10**, 1299.

SCHEIDEGGER, A. E. 1974 *The Physics of Flow Through Porous Media*. University of Toronto Press.

SMITH, F. T. & DUCK, P. W. 1977 *Q. J. Mech. Appl. Maths* **30**, 143.

SPALDING, D. B. 1972 *Intl J. Numer. Meth. Engng* **10**, 1299.

STEWARTSON, K. 1958 In *Boundary-Layer Research Symp. Freiburg*, p. 59. Springer.

WOODING, R. A. 1963 *J. Fluid Mech.* **15**, 527.

YAMAMOTO, K. 1974 *J. Phys. Soc. Japan* **37**, 1164.

YIH, C.-S. 1965 *Dynamics of Non-homogeneous Fluids*. Macmillan.